ADVANCED HEALTHCARE MATERIALS
www.advhealthmat.de

Lipid Nanoparticle-Mediated CRISPR-Cas13a Delivery for the Control of Bacterial Infection

Bookun Kim, Hwi Won Seo, Kyuri Lee, Dongeun Yong, Yoon Kyung Park, Yujin Lee, Solip Lee, Do-Wan Kim, Dajeong Kim, and Choong-Min Ryu**

Lipid nanoparticles (LNPs) can assist in the delivery of nucleic acid inside animal cells, as demonstrated by their use in COVID-19 vaccine development. However, LNPs applicable to bacteria have not been reported. Here, the screening of 511 LNPs containing random combinations of different lipid components identified two LNPs, LNP 496 and LNP 470, that efficiently delivered plasmids into *Escherichia coli* BW25113. Since Gram-negative bacteria have lipid bilayers, the bacteria are pretreated with LNP-helper that weakens the bacterial membrane. The cationic lipid DOTAP improved delivery of LNP-encapsulated plasmid DNA when present at a molar ratio of 10–25 mol% in the LNP. LNP encapsulation of the Cas13a/gRNA expression vector controlled infection by a clinical *Escherichia* strain in *Galleria mellonela* larvae and mouse infection models when used in combination with non-cytotoxic concentrations of polymyxin B, a bacterial membrane disruptor. Together, the results show that LNPs can be useful as a delivery platform for agents that counteract pathogenic bacterial infections.

1. Introduction

The over-prescription and misuse of antibiotics throughout the Coronavirus disease-19 (COVID-19) pandemic was commonplace because of the vulnerability of patients to secondary infection and the frequency of diagnostic uncertainty.[1] The overuse of antibiotics during the pandemic has contributed to the emergence and spread of antimicrobial resistant (AMR) bacteria.[2] In fact, antibiotic resistance could be considered a silent pandemic in itself.[3] While new antibiotics have been developed for AMR bacteria in recent decades, the occurrence of AMR bacteria has outpaced of development of these drugs.[4] Rising costs and slow progress in antibiotic development make it unlikely that the spread of AMR bacteria will be halted.[5] Indeed, investment into developing new antibiotics by pharmaceutical companies is continuously decreasing due to increasing costs of development and the rapid spread of antibiotic resistance.[2,5] In light of these challenges, alternative approaches to combating AMR bacteria are needed. Antibiotics alternatives include anti-virulence chemicals, probiotics, phages, host immune modulators, and quorum sensing inhibitors.[6] Another promising alternative is the delivery of nucleotide-based drugs inside bacterial cells, which could compensate for the stagnation in antibiotic development. The advantage of nucleotide-based drug delivery is that the drug can be designed to target specific genes such as virulence factors and antibiotic resistant genes.[7]

Previous studies have reported that the growth of AMR bacteria can be inhibited using the clustered regularly interspaced short palindromic repeats (CRISPR)-CRISPR-associated protein (Cas) system, such as Cas9,[8] dCas9[8] (catalytically inactive Cas9), Cas3,[9] and Cas13a.[10] While CRISPR-Cas9, CRISPR-dCas9, and CRISPR-Cas3 recognize the target site on genomic DNA, the CRISPR-Cas13a recognizes mRNA derived from genomic or plasmid DNA. This recognition is guided by a programmable guide RNA (gRNA). Cas13a catalyzes non-specific single-stranded RNA cleavage activity resulting in bacterial cell death.[10,11] However, an efficient and practical platform for the delivery of plasmids into the bacterial cytosol has not yet been developed.

To date, only a few delivery platforms targeting bacteria have been investigated, such as cell-penetrating peptides (CPPs), vitamin-B, and DNA nanostructures.[12] The general disadvantages of nucleic acid delivery systems include non-specific

B. Kim, H. W. Seo, Y. Lee, S. Lee, D.-W. Kim, D. Kim, C.-M. Ryu
Infectious Disease Research Center
Korea Research Institute of Bioscience and Biotechnology
Daejeon 34141, Republic of Korea
E-mail: djkim418@kribb.re.kr; cmryu@kribb.re.kr

K. Lee
College of Pharmacy and Research Institute of Pharmaceutical Sciences
Gyeongsang National University
Jinju 52828, Republic of Korea

D. Yong
Department of Laboratory Medicine and Research Institute of Bacterial Resistance
Yonsei University College of Medicine
Seoul 03722, Republic of Korea

Y. K. Park
Department of Biomedical Science
Chosun University
Gwangju 501–759, Republic of Korea

C.-M. Ryu
Department of Pediatrics School of Medicine
University of California at San Diego
La Jolla, CA 92093, USA

The ORCID identification number(s) for the author(s) of this article can be found under https://doi.org/10.1002/adhm.202403281

DOI: 10.1002/adhm.202403281

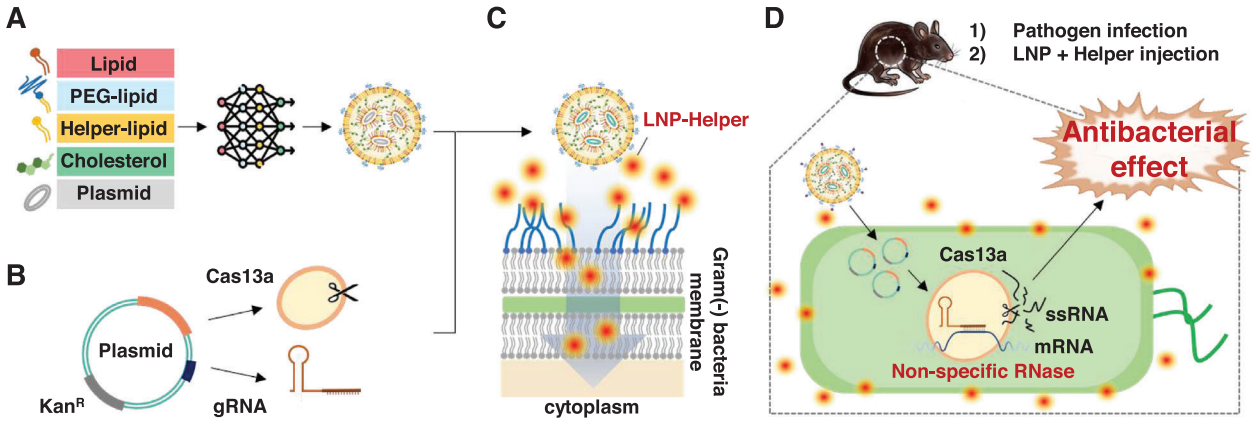

Figure 1. Schematic illustration of development of bacteria-targeting LNPs. A) Screening of LNP formulations with different components to deliver plasmids into bacterial cells. The LNP illustration is adapted from that of Swingle et al.[18] B) Cas13a protein and gRNA for target gene are expressed by one plasmid simultaneously. This plasmid is encapsulated by LNP. C) Before LNP treatment, "LNP-helper" is added to weaken the membranes of Gram-negative bacteria. D) To control bacterial infection in vivo, mice are infected with clinical isolate of *Escherichia fergusonii* intraperitoneally. Then, LNP and "LNP-helper" are also treated intraperitoneally. Delivery of LNPs into bacterial cells enables expression of the Cas13a protein and gRNA. Non-specific RNase activity of the Cas13a protein results in death of bacterial cells via degradation of ssRNA.

distribution, incomplete delivery within the cytoplasm, and organelle targeting.[13] Due to these issues, doubts have been raised about their therapeutic efficiency and side effects. For example, CPPs suffer from hemolysis side effects.[14] Additionally, the mass production and practical application of these platforms for practical usage have proven to be challenging.[12] Lipid nanoparticles (LNPs) have great potential for the delivery of mRNA to eukaryotic cells, as demonstrated by their use in mRNA vaccines.[15] The advantages of LNP-based mRNA vaccines have been evaluated in terms of stability, productivity, rapid development, and unit cost.[16] Moreover, advantages of LNPs also include efficient encapsulation of genetic material, enhanced cellular uptake, and reduced immunogenicity, making them a highly favorable option for future therapeutic applications compared with previous nanocarriers such as liposomes.[17] Overall, the success of LNPs in recent years marks a pivotal shift in the landscape of drug delivery technologies.

However, to date, no LNP-based mRNA or DNA delivery systems have been applied to bacteria, although they potentially represent a promising and innovative substitute for other delivery systems to AMR bacteria. The rapid development capability of LNP makes them suitable for targeting AMR bacteria. In this study, we developed bacteria-targeting LNPs with the aim of controlling *Escherichia*-derived sepsis in vivo (**Figure 1**). We screened LNPs for their ability to deliver efficiently a Cas13a/gRNA expression vector into bacterial cells. We found that "LNP-helpers" capable of weakening the bacterial outer membrane are essential for the delivery of LNPs. When the gRNA was designed to recognize the 16s ribosomal RNA (rRNA) gene, the LNP-encapsulated Cas13a/gRNA expression vector controlled pathogenic bacteria infection in mouse and *Galleria mellonela* infection models.

2. Results

2.1. Screening of LNP Combinations for Plasmid Delivery Into Bacteria

Different LNPs with different combinations of lipids were tested for their ability to deliver plasmid DNA into bacteria using a novel screening system (**Figure 2A**). Because no information was available about the optimal LNP composition required for the delivery of plasmids into bacterial cells, we tested LNPs with different lipid combinations, including lipidoid, helper lipid, cholesterol, and PEG-lipid (Table S1, Supporting Information). *Escherichia coli* strain BW25113 was incubated with each plasmid DNA-containing LNP and then the bacterial cells were spread on a Luria-Bertani (LB) agar plate containing ampicillin (Amp) to select for those receiving the plasmid DNA. The plasmid used in this study was pAD123::INR7, which expresses the Amp resistance gene and enhanced green fluorescent protein (EGFP) under the control of a strong constitutive promoter. After delivery of this plasmid into *E. coli* BW25113, the number of bacterial colonies showing EGFP expression was counted on an LB agar plate containing 50 μg mL^{-1} ampicillin to confirm LNP-mediated delivery of pAD123::INR7, as shown in Figure 2A. Table S1 (Supporting Information) shows the LNP formulations that were screened in vitro to determine which LNPs efficiently delivered the plasmid into the bacterial cells. When delivery of the plasmid DNA by LNPs was achieved, viable EGFP-positive colonies could be identified on antibiotic agar plates. In fact, all colonies that survived on antibiotic agar plates simultaneously exhibited fluorescence when measured by a non-UV illuminator. Statistically significant results were not obtained for LNP 1 to 460, because the number of bacteria cells that received the plasmid was below 300 CFU mL^{-1} from LNP 1 to 460 (Figure S1A, Supporting Information).

2.2. Introduction of a Membrane Disruptor

We hypothesized that the membrane structure of Gram-negative bacteria, which is characterized by a lipid bilayer and a peptidoglycan cell wall,[19] may have prevented the efficient delivery of the LNP-encapsulated plasmid (Figure S1A, Supporting Information). Therefore, bacteria cells were pretreated with a lipopeptide antibiotic, polymyxin B (PMB), because the net positive charge of PMB is known to facilitate its binding to negatively charged lipopolysaccharide (−35 to −45 mV)[20] (LPS), thereby

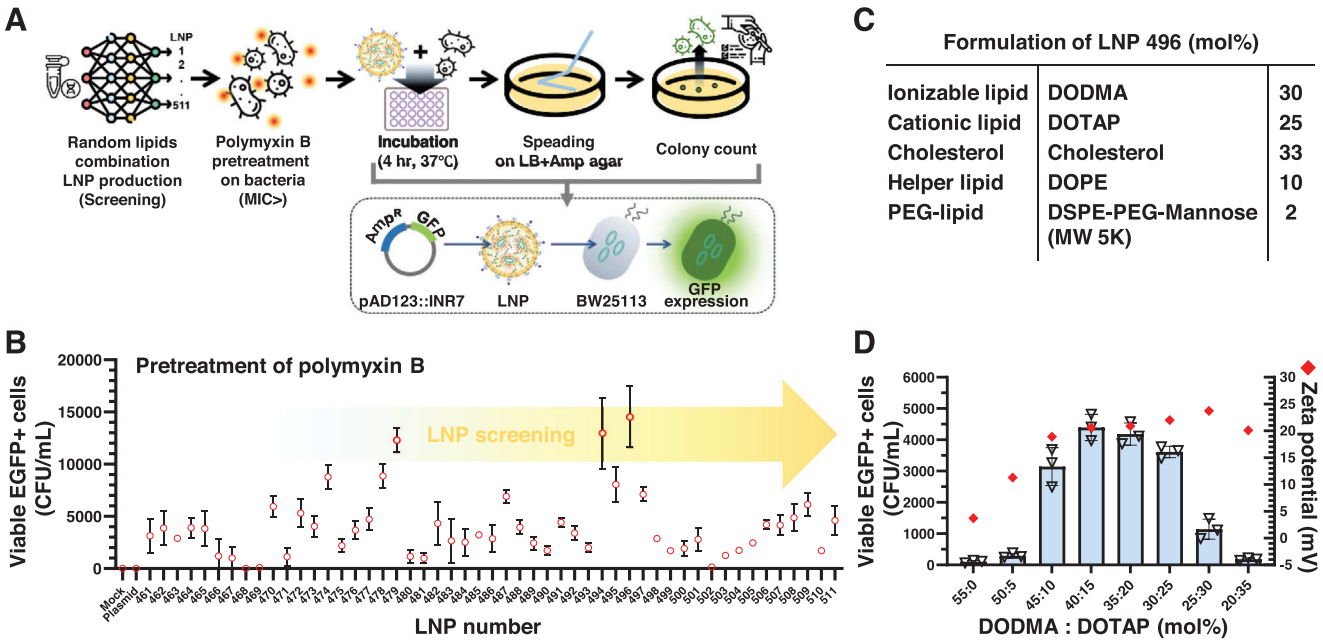

Figure 2. Screening and characterization of the LNPs used to treat bacteria. A) Schematic illustration of the experimental method used to screen whether an LNP can deliver the EGFP-encoding plasmid (pAD123::INR7) into *E. coli* BW25113. LNPs used to encapsulate plasmids were prepared by rapid hand mixing using random combinations of different lipids. *E. coli* bacterial cells were pretreated with polymyxin B (PMB) and then incubated with each LNP in a 96 multi-well plate. The mixture was then spread on LB agar medium containing ampicillin (Amp) and incubated. Finally, colonies expressing EGFP on the agar plate were counted as viable cells (CFU mL^{-1}). B) Using the screening method depicted in Figure 2A, the delivery of plasmids using LNP 461–511 was evaluated by counting the number of colonies expressing EGFP. *E. coli* BW25113 was pretreated with PMB at a concentration of 1.5 μg mL^{-1} before LNP treatment. Experiments were performed in triplicate and presented as mean ± SD. As a negative control, bacterial cells were treated with PBS or plasmid DNA instead of LNP-encapsulated DNA (mock and plasmids, respectively). C) Composition of LNP 496. LNP 496 was formulated with DODMA, DOTAP, cholesterol, DOPE, and DSPE-PEG-Mannose (molecular weight 5000) at a molar ratio of 30:25:33:10:2. D) LNP delivery was evaluated in triplicate and presented as mean ± SD using the number of colonies according to the mol% ratio of ionizable lipid DODMA and cationic lipid DOTAP in LNP 470. The zeta potential value of each LNP formulation was determined using dynamic light scattering (DLS) analysis in triplicate and presented as mean.

weakening bacterial membranes at concentrations lower than the minimum inhibitory concentration (MIC) of 4 μg mL^{-1}.[21] When we applied PMB as a membrane-weakening agent during the screening from LNP 461 to 511, PMB pretreatment resulted in a dramatic increase in the number of colonies (Figure 2B). Since screening of LNP 1 to 460 was performed without PMB pretreatment, representative LNP formulations with different compositions from LNP 1 to 511 were selected and their delivery efficiency in the presence of PMB was then evaluated (Figure S1B, Supporting Information). PMB pretreatment increased plasmid delivery only when LNPs with numbers higher than 461 were used (Figure S1B, Supporting Information; Figure 2B). To exclude the possibility that plasmid DNA itself could be transferred to bacterial cells under PMB pretreatment, we tested a group only treated with bare plasmid DNA in the LNP screening experiment. However, plasmid DNA was not transferred. (Figure 2B). For LNP 496, the average number of bacterial cells that received the plasmid was 14520 CFU mL^{-1} (Figure 2B,C). Hereafter, we refer to PMB and other bacterial membrane disruptors as "LNP-helpers". Polymyxins are lipopeptide antibiotics that disrupt the outer membrane of bacteria. As expected, in addition to polymyxin B, polymyxin E (colistin) increased LNP delivery at concentrations lower than its MIC (Figure S1C, Supporting Information). Additionally, antimicrobial peptide 2 (AMP2) and a synthetic nitrophenol compound PA108[22] increased the delivery efficiency of LNP 496 (Figure S1D, Supporting Information), indicating that pretreatment with an "LNP-helper" increases the efficiency of LNP-mediated nucleic acid delivery into bacteria.

2.3. Evaluation of LNP Delivery According to the Molar Ratio of Cationic Lipid in LNP Composition

Considering representative LNP formulations in Figure S1B (Supporting Information), the use of ionizable lipids and cationic lipids together enabled the delivery of LNPs to bacteria. Thus, we evaluated the plasmid delivery efficiency of LNP 470 by varying the molar ratios of DODMA (an ionizable lipid) to DOTAP (a cationic lipid) (Figure 2D). When DODMA and DOTAP were present at a molar ratio of 30:25, the zeta potential measured was +22 mV (Figure 2D). Plasmid delivery was optimal with DOTAP present at 10–25 mol% (Figure 2D). However, although electrostatic potential remained highly positive at molar ratios of 25:30 and 20:35, plasmid delivery was lower at these ratios (Figure 2D) suggesting that while DOTAP was predicted to possess an electrostatic potential favorable for LNP delivery, high

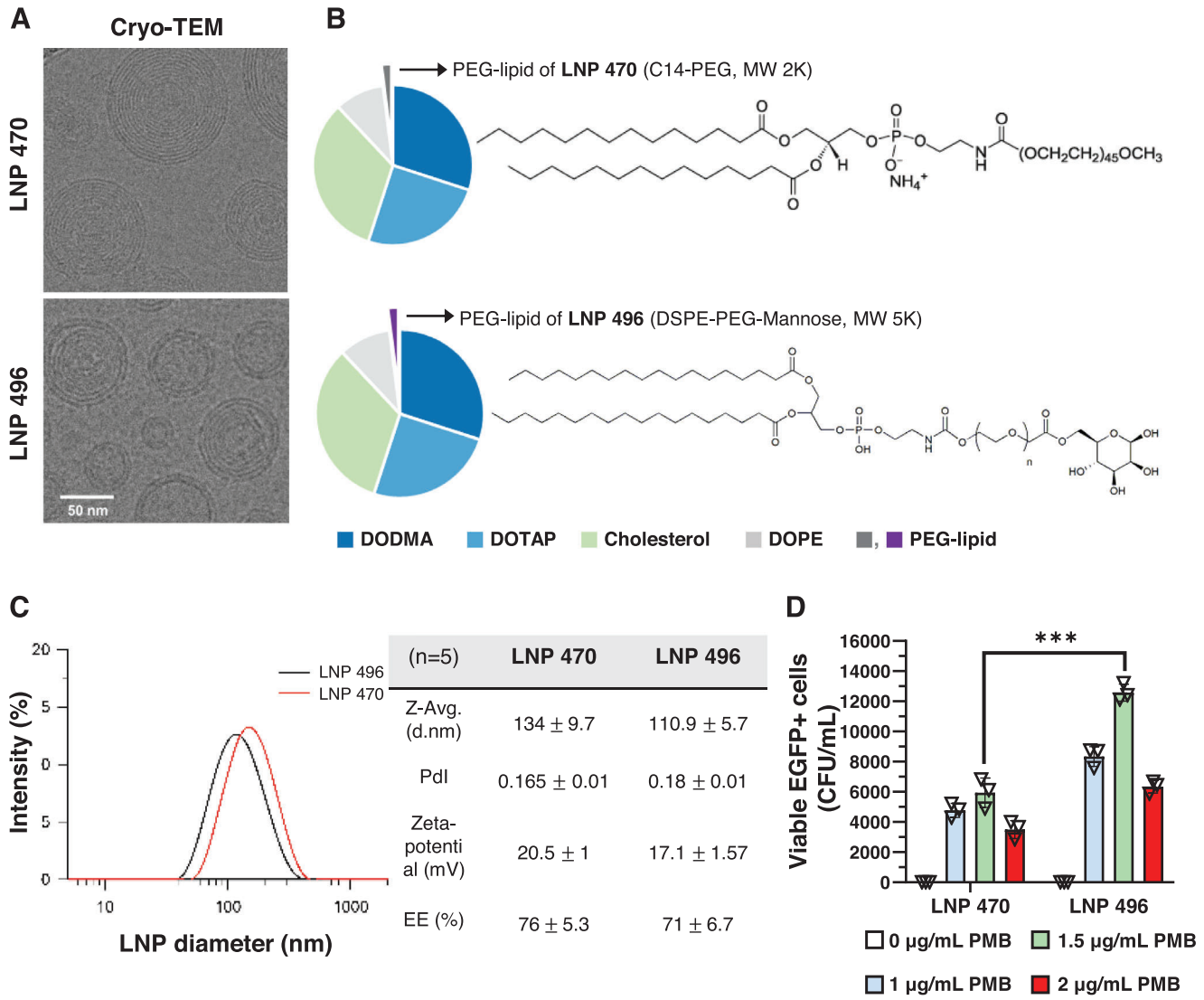

Figure 3. Comparison of LNP 470 and LNP 496. A) LNP 470 and LNP 496 were examined using cryo-transmission electron microscopy (cryo-TEM). B) Components and molar ratio (mol%) of lipids in the two LNPs are depicted as pie charts. The ratios of DODMA, DOTAP, cholesterol, DOPE, and PEG-lipid in the two LNPs were 30:25:33:10:2, as shown in Figure 2C. The PEG-lipids of LNP 470 and LNP 496 are presented with their chemical structures. C) The diameters (d.nm), polydispersity index (PdI), and Zeta-potential of the LNPs were measured at 20.0 °C by DLS analysis. Encapsulation efficiency (EE %) was determined via PicoGreen dsDNA assay. Data were shown in the table with mean ± SD of sample size $n = 5$. D) LNP 470- and LNP 496-mediated plasmid delivery were determined after pretreatment of the *E. coli* bacterial cells with 0, 1, 1.5, and 2 μg mL^{-1} of PMB. After LNP treatment, the number of bacterial cells conveying the plasmid on the plate was counted (CFU mL^{-1}). The error bars represent the mean ± SD with n = 3 sample size. *P* values were determined using two-tailed Student's t-test ($^{***}p < 0.001$).

proportions of DOTAP may not help deliver LNPs stably to the bacterial cytoplasm.[23]

2.4. Rheological Study of LNPs

We adopted a rheological approach to analyze the electrostatic interactions between LNPs and bacteria (Figure S2, Supporting Information). Shear viscosity (Figure S2A, Supporting Information) was measured, and the overall effective volume fraction ϕ_{eff} value was estimated (Figure S2B, Supporting Information) using Batchelor's equation[24] for semi-dilute dispersion (hard sphere), which is given by the formula $\eta_r = \eta_0 / \eta_s = 1+2.5\phi_{eff}+5.9\phi_{eff}^2$ (η_r: relative viscosity, η_0: zero shear viscosity, η_s: solvent viscosity). The effective volume fractions of LNP 470 were 0.095 in 1X phosphate-buffered saline (PBS) and 0.13 in deionized (DI) water, respectively (Figure S2B, Supporting Information), indicating that ions in PBS reduced the effective volume of the particles and consequently, their electrostatic radius.[25] We assessed the plasmid delivery efficiency of LNP 470 under different ion conditions represented by distilled water (DI) and 1X PBS. The delivery of LNPs into bacteria was significantly higher (average (AVG) 4810 CFU mL^{-1}) in DI water compared to 1X PBS (AVG 289 CFU mL^{-1}) (Figure S2C, Supporting

Information). This result suggests that the electrostatic radius of the LNP influences the efficiency of nucleic acid delivery.

2.5. Comparison of Delivery Efficiency Between LNP 496 and LNP 470

Characteristics of LNP 496 and 470 were determined using cryo-TEM imaging and dynamic light scattering (DLS) (**Figure 3A,C**). LNP 496 and LNP 470 exhibit positive zeta-potentials (17.1 and 20.5 mV, respectively), small sizes (110.9 and 134 nm, respectively), and acceptable polydispersity indexes (PdI; 0.18 and 0.165, respectively) (Figure 3C). Moreover, the encapsulation efficiency (EE, %) was 76% for LNP 470 and 71% for LNP 496 (Figure 3C). LNP 496, which resulted in the highest plasmid delivery efficiency (Figure 1B, AVG 14520 CFU mL^{-1}), and LNP 470 share the same composition, except for a difference in their PEG-lipid content (Figure 3B). The PEG-lipid content of LNP 496 was 2 mol% DSPE-PEG-mannose (molecular weight 5000 (MW 5K), indicating that mannose is exposed on the surface of LNP 496. Previously, mannose was reported to attach to a mannose specific lectin protein FimH on the surface of E. coli,[26] suggesting that mannose on the surface of LNPs could enhance LNP-mediated plasmid delivery into bacteria. Indeed, the plasmid delivery efficiency of LNP 496 was significantly increased compared to that of LNP 470 at a PMB concentration of 1.5 μg mL^{-1} (Figure 3D). In this experiment, when we calculated the ratio of the number of bacterial cells delivered with plasmids to the total number of bacterial cells, the delivery efficiency of LNPs was calculated to be up to 0.00038% (Figure S3, Supporting Information). To exclude the possibility that LNPs may have an antibacterial effect, we measured the antibacterial effect of LNPs at a PMB concentration of 2 μg mL^{-1}. When we determined the number of total viable cells before and after the treatment of LNPs, LNPs did not cause bacterial cell death (Figure S4, Supporting Information).

2.6. Delivery of LNPs to Gram-Negative and Gram-Positive Bacteria

We also evaluated the efficiency of plasmid delivery by LNP 496 into other bacteria species (**Figure 4A**). LNP-encapsulated plasmids were delivered only to the other Gram-negative bacteria *Shigella sonnei*, *Citrobacter freundii*, and *Klebsiella pneumoniae* (Figure 4A), indicating that LNP-mediated plasmid delivery is applicable to other Gram-negative pathogenic bacteria species except *Salmonella* Typhimurium. However, LNP-encapsulated plasmids were not delivered to Gram-positive bacteria, even in the presence of daptomycin, an "LNP-helper" that disrupts the membranes of Gram-positive bacteria (Figure 4A).

2.7. LNP-Mediated Plasmid Delivery to Animal Cells

LNP 470 and LNP 496 did not affect the cell viability of the human epithelial cell line HeLa and the human embryonic kidney cell line HEK293T (Figure 4B), suggesting that they lack toxicity toward human cells. To test LNP delivery into human cell lines, we encapsulated EGFP mRNA using LNP 470 or LNP 496. LNP 470 and LNP 496 delivered EGFP mRNA into the tested cell lines as effectively as the Moderna LNP (Figure 4C).

2.8. Potential for the Control of Pathogenic Bacteria Using LNP-Encapsulated Plasmid DNA Expressing Cas13a and gRNA Targeted to 16s Ribosomal RNA

Next, we investigated whether LNPs could be used to prevent infections caused by pathogenic bacteria. To determine the virulence of the clinical isolates obtained from sepsis patients, we infected *Galleria mellonella* caterpillars with each of 15 clinical isolates from sepsis patients and determined survival rates of *G. mellonella* after infection. Among the isolates, 12 exhibited higher virulence than *E. coli* BW25113 (**Figure 5A**). Since 12 isolates were resistant to ampicillin (Figure S7, Supporting Information), we used chloramphenicol selection, another antibiotic marker of the pAD123::INR7 plasmid, to confirm plasmid DNA delivery by LNP 470 and LNP 496. Among 12 highly pathogenic isolates, 10 strains with chloramphenicol resistance were selected (Figure S7, Supporting Information). LNPs were delivered to 40% of clinical isolates (Figure 5B). In addition to PMB, the "LNP-helper" PA108 and AMP2 increased nucleic acid delivery by LNPs into isolate no. 23 (Figure 5C). To inhibit bacterial growth, we employed the CRISPR-Cas13a system (**Figure 6A**), which recognizes target RNA sequences with the help of gRNA and cleaves non-specific RNAs leading to cell death (Figure 6A,B). For this purpose, we prepared plasmids expressing Cas13a and Cas13a-gRNA, which targets 16s ribosomal RNA of Escherichia strains,[27] and used them to treat E. fergusonii isolate no. 23 after their encapsulation by LNP496. LNP 496-Cas13a and LNP 496-Cas13a-gRNA resulted in colony counts of 2020 and 480 CFU mL^{-1}, respectively (Figure 6C), suggesting that the non-specific RNase activity of the Cas13a protein caused cell death in of isolate no. 23 (Figure 6B). Moreover, when bacterial cells were treated with LNP 496-Cas13a-gRNA, the amount of total RNA decreased compared to when treated with LNP 496-Cas13a. This result also supports that a non-specific RNase activity of Cas13a degraded bacterial total RNA when gRNA was elicited (Figure S5, Supporting Information). We next examined the effects of LNP-Cas13a-gRNA on the survival of mouse and *G. mellonella* caterpillars infected with *E. fergusonii* isolate no. 23 (Figure 6D–F). In *Galleria mellonella* infected with *E. fergusonii* isolate no. 23, we first determined the efficacy of LNPs according to the presence or absence of LNP-helper (PMB) and the presence or absence of gRNA in CRISPR system. The survival rates of *G. mellonella* was 40% only when PMB was treated to bacteria and LNPs delivered plasmid encoding Cas13a/gRNA together (Figure 6D). Moreover, when we compared LNP 470- and LNP 496-Cas13a-gRNA with LNP 496-Cas13a, the survival rates were 0% for LNP-Cas13a and 20%–30% for LNP-Cas13a-gRNA after 48 h (Figure 6E) indicating that delivery of both Cas13a and gRNA resulted in therapeutic effect. In the mouse infection model, injection with LNP496-Cas13a or LNP496-Cas13a-gRNA resulted in survival rates of 10% or 70% after 80 h, respectively (Figure 6F). These results suggest the therapeutic potential of Cas13a-gRNA encapsulated in LNPs for the treatment of bacterial infection.

3. Discussion

In this study, we prepared LNPs with different lipid compositions to identify LNPs capable of delivering nucleic acids efficiently

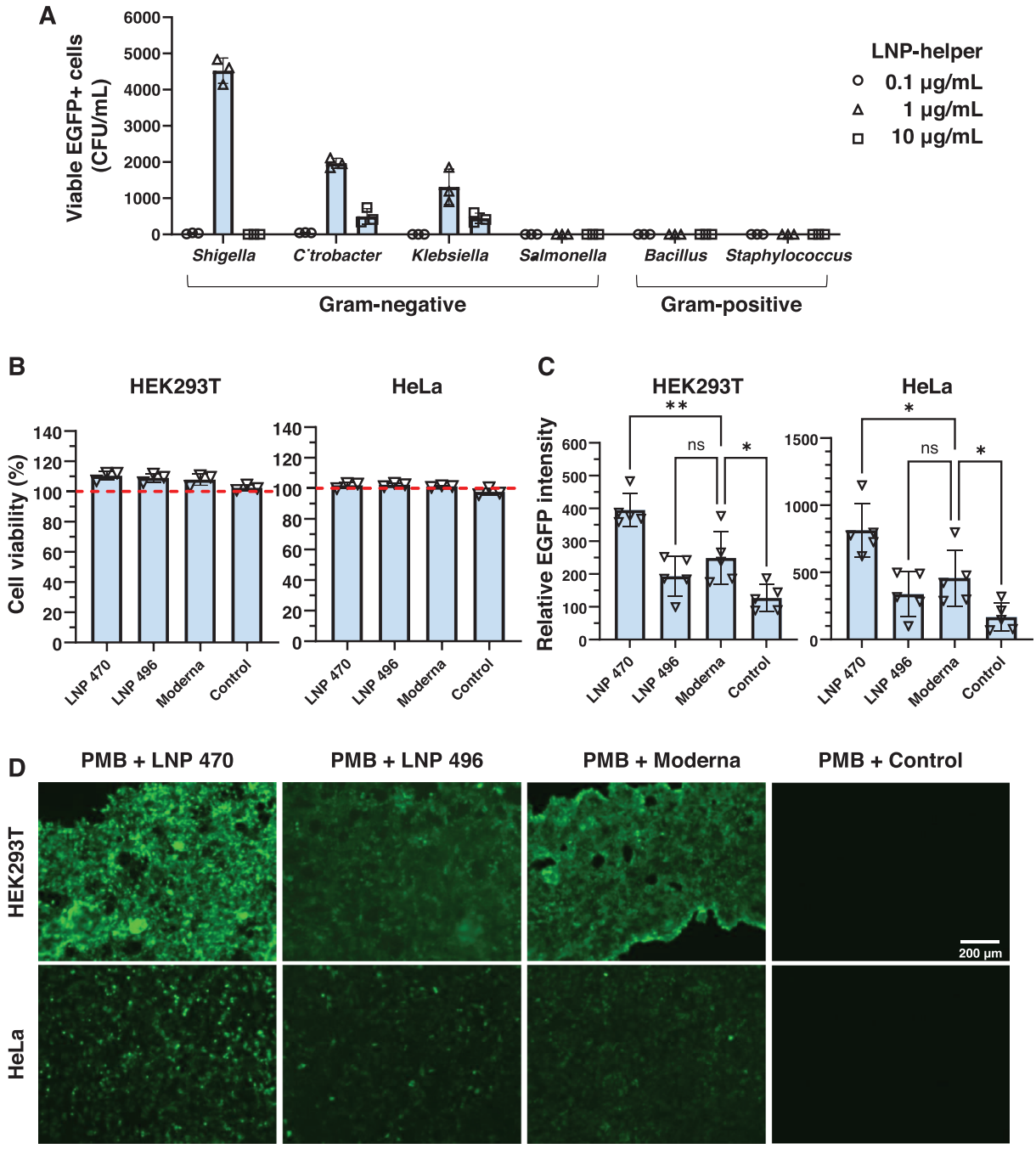

Figure 4. Delivery efficiency of LNPs into other bacteria species and human cell lines. A) The plasmid delivery of LNP 496 was evaluated in the Gram-negative species *Shigella sonnai* (*Shigella*), *Citrobacter freundii* (*Citrobacter*), *Klebsiella pneumoniae* (*Klebsiella*), and *Salmonella* Typhimurium (*Salmonella*), and the Gram-positive bacteria *Bacillus subtilis* (*Bacillus*) and *Staphylococcus aureus* (*Staphylococcus*). Prior to LNP treatment, the bacteria were treated with an "LNP-helper" at the indicated concentrations. After LNP treatment, the number of bacterial cells conveying the plasmid on the plate was counted (CFU mL^{-1}). Polymyxin B and daptomycin were used for Gram-negative and Gram-positive bacteria, respectively. The error bars represent the mean ± SD with $n = 3$ sample size. B,C) Cytotoxicity and plasmid delivery efficiency of LNPs were determined using HEK293T and HeLa cell lines 24 h after LNP treatment. Both animal cells were cultured in 24 multi-well plates at a density of 1×10^5 CFU mL^{-1} and pre-incubated for 24 h. The pre-incubated cells were transfected with 100 ng of mRNA using either Lipofectamine 3000 transfection reagent or LNPs. EGFP mRNA was encapsulated with LNP 470, LNP 496, or the Moderna formulation. Moderna LNP was used as positive control. As a negative control, cell lines were treated with PBS (Control). Cell viability relative to the control was calculated for each cell line ($n = 3$). Relative EGFP mRNA expression was normalized to the level of control, which was set at 100% ($n = 5$). Data are shown as mean ± SD. *P* values were determined using ANOVA, followed by Dunnett's multiple comparisons test (ns, not significant; $^{*}p < 0.05$, $^{**}p < 0.01$). D) Representative fluorescence microscopy images were used to abstract the data shown in Figure 4B,C. HEK293T and HeLa cells were treated with LNP-encapsulated EGFP mRNA. PMB was also added at a concentration of 1 µg mL^{-1} in DMEM media before LNP treatment. Scale bar, 200 µm.

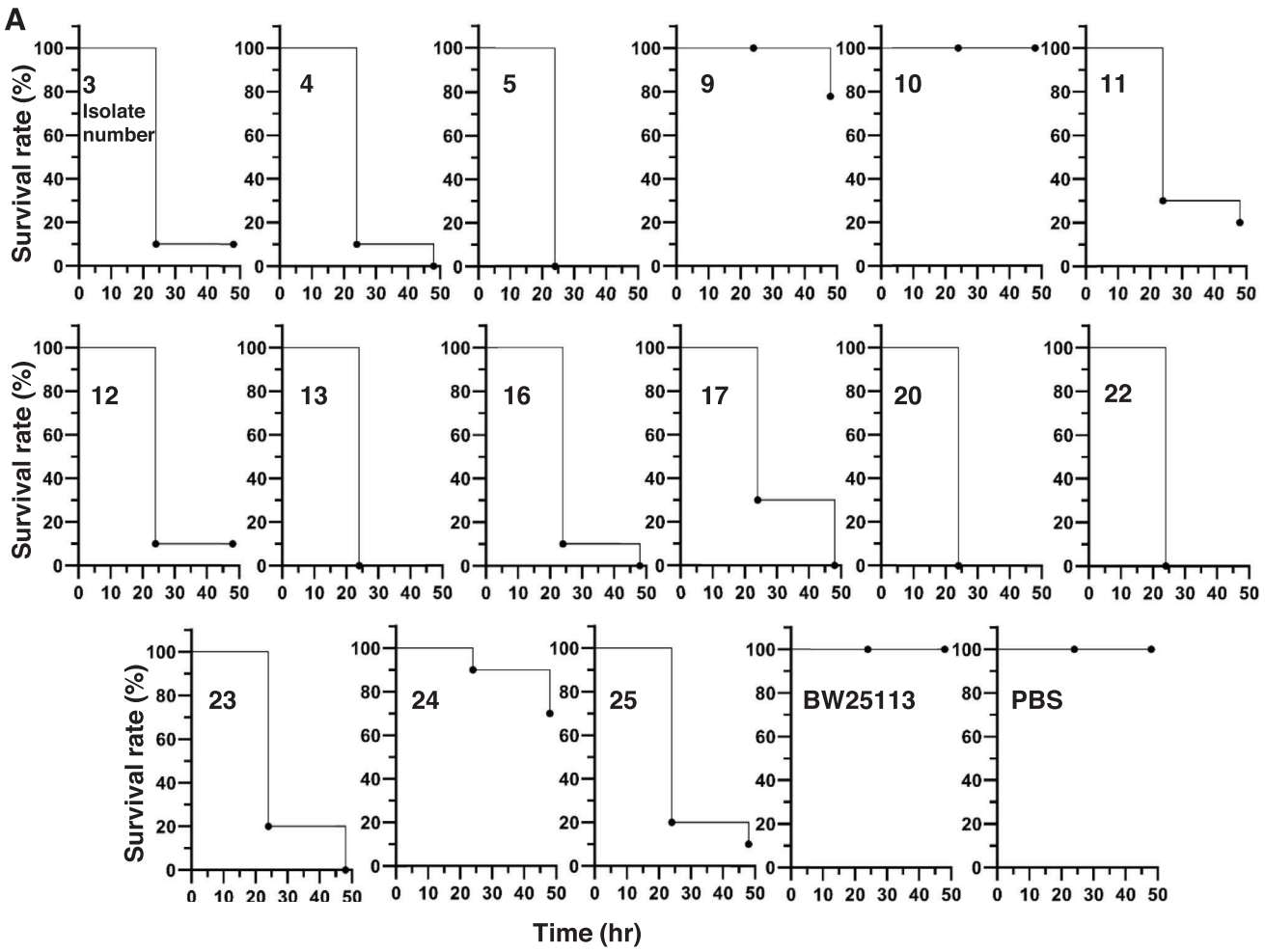

Figure 5. Treatment of *Galleria mellonella* caterpillars infected with *Escherichia* isolates from sepsis patients with LNP-encapsulated pAD123::INR7 plasmid. A) Time to death of *Galleria mellonella* caterpillars infected with various *Escherichia* isolates from sepsis patients. 10 μL of bacterial culture (1.0×109 CFU mL^{-1}) was injected into *G. mellonella* caterpillars ($n = 10$) using insulin syringes. Survival rate of *G. mellonella* caterpillars was determined during the indicated period. *E. coli* BW25113 was used as a negative control. B) LNP-mediated plasmid delivery into the clinical isolates was evaluated. All isolates were pretreated with 2 μg mL^{-1} PMB. The efficiencies of LNP 470- and LNP 496-mediaetd delivery of pAD123::INR7 plasmid were determined by counting colonies on chloramphenicol plates. C) Plasmid delivery of LNP 496 according to the concentrations of "LNP-helper" (PMB, PA108, and AMP2). Isolate no. 23 was pretreated with each "LNP-helper" at the indicated concentrations. For B and C, experiments were performed in triplicate and presented as mean ± SD.

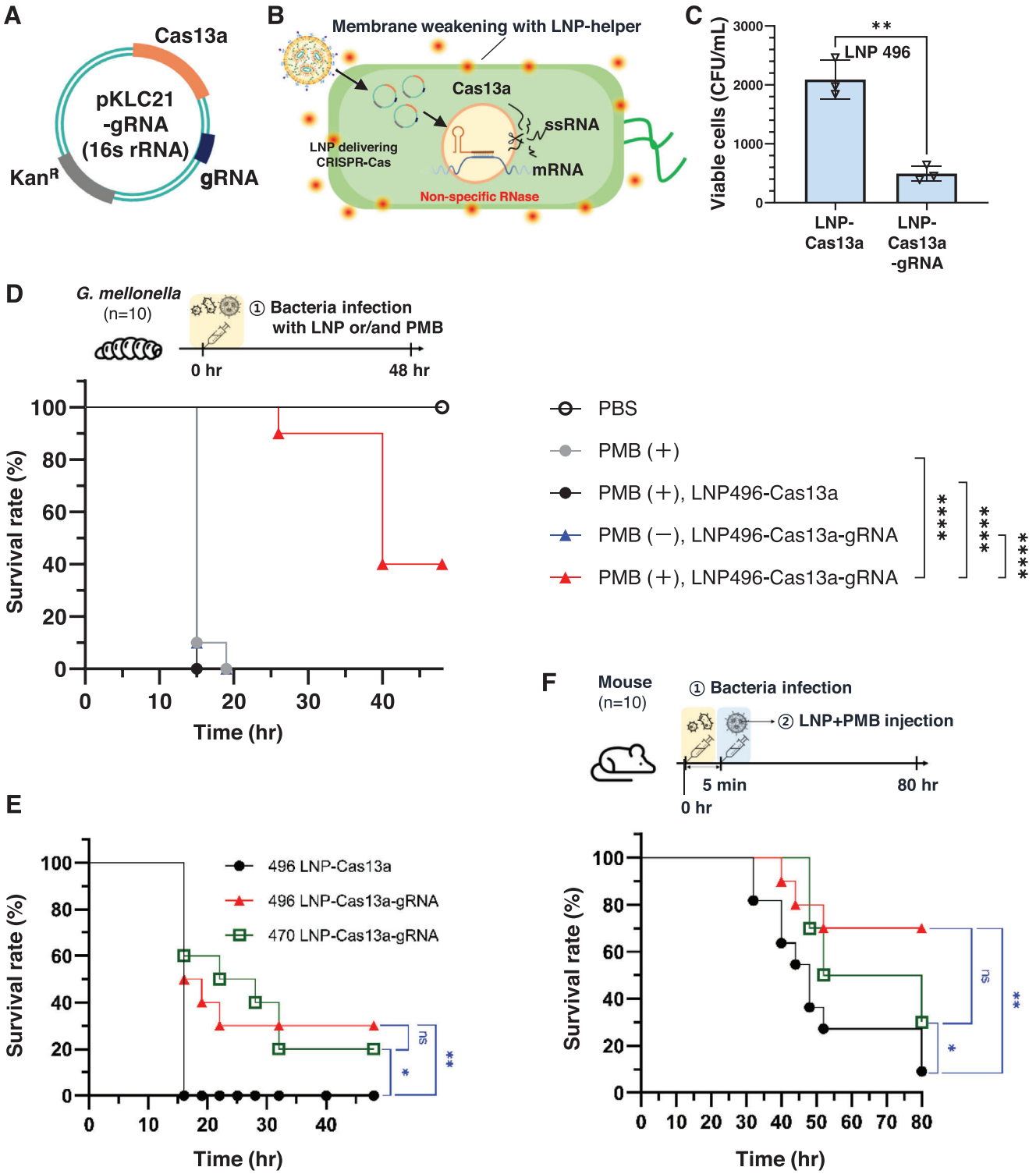

Figure 6. LNP-mediated CRISPR-Cas13a delivery for the control of infection caused by a clinical isolate of *Escherichia fergusonii*. A) Schematic diagram of the plasmid expressing Cas13a and gRNA for the targeting of the 16s rRNA gene of *Escherichia coli*. The kanamycin resistant gene (Kan^R) on the plasmid was used for selection. B) Schema illustrating of the mechanism of LNP-mediated CRISPR-Cas13a delivery. The gRNA recognizes the target gene and Cas13a/gRNA complex cleaves the gene. The Cas13a protein also has non-specific RNase activity. The illustration of CRISPR-Cas13a activity is adapted from that of Kiga et al.[28] C) Bacteria-killing resulting from the LNP496-mediated delivery of the Cas13a gene was determined for the clinical isolate no. 23. Plasmids encoding Cas13a or Cas13a/gRNA were encapsulated with LNP 496 (LNP-Cas13a and LNP-Cas13a-gRNA, respectively). Isolate no. 23 was pretreated with 2 μg mL^{-1} PMB before LNP treatment. The error bars represent the mean ± SD ($n = 3$). Data was analyzed by two-tailed

into bacteria cells. The LNPs were composed of different ratios of a neutral structural lipid, ionizable lipid, cholesterol, and a PEG-lipid.[29] We produced 511 LNPs with various ratios of 19 ionizable lipids or cationic lipids, six helper lipids, and 10 PEG-lipids (Table S1, Supporting Information). We found that LNP 496 had the highest delivery efficiency among the various LNPs tested. LNP 496 consists of DODMA, DOTAP, cholesterol, DOPE, and DSPE-PEG-mannose (Figure 2C). In particular, the introduction of DOTAP, a cationic lipid, increased the efficiency of plasmid delivery into *E. coli*. It is possible that the positive charge of LNP 496 conferred by DOTAP complemented the negative charge of the peptidoglycan layer of *E. coli* cells, thereby increasing the mobility of the LNP on the bacterial surface. However, delivery efficiency decreased when we increased the positive charge of the LNP 496 by changing the molar ratio of DODMA:DOTAP from 30:25 to 25:30 or 20:35 (Figure 2D). Interactions between the lipids of LNPs and cellular membranes are known to be important factors in LNP delivery.[23,30] Because DOTAP is known to result in the loss of mammalian cell viability,[31] we speculated that the increase in the ratio of this lipid in LNP 496 resulted in low plasmid delivery efficiency was because it caused loss of bacterial cell viability. However, no bacterial death was observed when *E. coli* cells were treated with LNPs containing 30 and 35 mol% DOTAP (data not shown).

Chemicals, peptides, proteins, antibodies, carbohydrates, and vitamins can be used as targeting ligands on the surface of LNPs to enhance their delivery into cells.[32] Targeting ligands that specifically bind to receptors differentially expressed in each tissue can enhance internalization of LNPs into animal cells through receptor-mediated endocytosis.[32] We found that LNP 496 is composed of DSPE-PEG-mannose, a PEG-lipid that serves as a targeting ligand on the surface of its surface (Figure 3B). Recent studies have reported that DSPE-PEG-mannose increases LNP delivery into immune cells,[33,34] which utilize a mannose receptor for pathogen recognition.[35] In the case of bacteria, the mannose phosphotransferase system (PTS) mediates mannose uptake, and mannose permeases of the PTS are involved in sugar recognition.[36,37] Moreover, according to structural research by Hung et al., the FimH tip protein in type I pili of *E. coli* can enclose mannose molecules within a deep pocket.[38] Bouckaert et al. demonstrated that mannose exhibits a much higher affinity for FimH than for glucose and fructose.[39] We speculated that the mannose particles exposed on the surface of LNP 496 would enhance LNP 496 delivery into bacteria by binding to mannose permeases or FimH on the bacterial surface. In contrast, our results showed that LNP 496 did not enhance LNP uptake in mammalian cells (Figure 4C). Collectively, the screening data provide valuable insights into the potential benefits of mannose on LNPs for targeting bacteria.

We found that pretreatment with an "LNP-helper" increased the efficiency of LNP-mediated plasmid DNA delivery into bacteria. Unlike animal cells, the bacterial cell membrane is protected by additional protective structures. Gram-negative bacteria have a thin peptidoglycan layer and an outer membrane surrounding the inner membrane, while Gram-positive bacteria have a thick layer of peptidoglycan covering the outer surface of the inner membrane. We hypothesized that weakening the outer membrane of Gram-negative bacteria would increase LNP delivery efficiency. A recent study suggested that polymyxin treatment creates an LPS-polymyxin crystal structure in the membrane of *E. coli* that results in membrane disruption.[40] Indeed, we found that a PMB concentration lower than its minimum inhibitory concentration increased LNP delivery (Figure 3D). While polymyxin is a lipopeptide that targets bacterial membranes, small peptide AMPs have been reported to inhibit the survival of bacteria, fungi, parasites, and viruses.[41] In particular, AMPs with a direct bactericidal mechanism can bind to negatively charged bacterial membranes, creating holes in the membrane or controlling the permeability of the membrane.[41,42] We tested three AMPs with bactericidal effects to determine whether they could act as "LNP-helper", as well as PA108, a compound that weakens the membrane of Gram-negative bacteria. Among the compounds, AMP2 and PA108 acted as "LNP-helper" (Figure 5C; Figure S1D, Supporting Information), suggesting that compounds that alter bacterial membrane permeability could be effective as "LNP-helper". Further development of LNP-helpers could enhance the potential of LNP applications.

LNP 496 and LNP 470 were also efficient for delivering plasmid DNA into other Gram-negative bacteria, including *Shigella*, *Citrobacter*, and *Klebsiella* strains, excluding *Salmonella* Typhimurium (Figure 4A). A significant difference between the outer membranes of *E. coli* and *S. Typhimurium* is the composition of lipid A in the lipopolysaccharide that forms the outer membrane (Figure S6, Supporting Information). Several pathogens, including *Salmonella*, utilize lipid A modifications to evade the host immune system and promote pathogenesis.[43] *Salmonella*, unlike *E. coli*, adds 4-amino-4-deoxy-L-arabinose and phosphoethanolamine to lipid A (Figure S6, Supporting Information), and these modifications alter the net negative charge of the outer membrane.[44,45] It was possible that the difference in membrane charge between *E.coli* and *S. Typhimurium* cell membranes reduced the ability of *E. coli*-optimized LNP 496 or LNP 470 to access the surface of *S. Typhimurium*, thereby hindering LNP-mediated plasmid delivery into *Salmonella*. Moreover, LNP

Student's *t*-test ($^{**}p < 0.01$). D,E) In vivo efficacy of LNP-Cas13a-gRNA in the *G. mellonella* infection model. *G. mellonella* caterpillars ($n = 10$) were inoculated with mixture of isolate no. 23 culture, LNP 496 or LNP 470, and PMB. (D) Survival rates of *G. mellonella* caterpillars infected with clinical isolate No. 23 (9.5×10^6 CFU/caterpillar) were determined under different treatments for 48 h. The red and blue triangles indicate the treatment of LNP 496 encapsulating plasmids encoding Cas13a and gRNA (LNP 496-Cas13a-gRNA) with or without the treatment of polymyxin, respectively (PMB (+) and PMB (-)). LNP 496 encapsulating plasmid encoding only Cas13a (LNP 496-Cas13a) was used as a control (black circle). The group treated with PBS instead of bacterial infection was used as a negative control (white circle), and the group treated with PMB only was used as a positive control (gray circle). In the graph, the blue triangles are obscured by gray circles. F) In the mouse infection model, mice ($n = 10$) were injected intraperitoneally with a mixture of LNP 496 or LNP 470 and PMB 3 min after injection with isolate no. 23 (2.4×10^8 CFU/mouse). Survival rates of mice were determined during the indicated time periods. For survival experiments (D–F), *P* values were determined using the Log-rank (Mantel-Cox) t-test (ns, not significant; $^{*}p < 0.05$, $^{**}p < 0.01$, $^{***}p < 0.001$, $^{****}p < 0.0001$).

delivery was effective against only 40% of pathogenic *E. coli* isolates (Figure 5B). We speculate that this may be due to differences in lipid A modifications among strains, based on a recent report that pathogenic *E. coli* strains acquire genes related to lipid A modification through plasmid transfer.[46]

The CRISPR-Cas system is a promising gene-editing tool that can be exploited to control bacterial infections. Cas9, a bacterial RNA-guided endonuclease, cuts genomic DNA at locations that correspond to RNA recognition sequences.[47] Recent studies demonstrated that the CRISPR-Cas9 complex can be used to modify target genes in order to eliminate specific bacterial strains.[48–50] CRISPR-Cas13a has also been developed for its non-specific single-stranded RNA (ssRNA) cleavage activity.[28] In the study by Kiga et al., the recognition of target AMR genes by the Cas13a protein activates its promiscuous ssRNA activity, leading to bacterial cell death.[28] However, a major stumbling block in using this methodology to block bacterial infections is the delivery platform for the CRISPR-Cas system into bacteria. To date, platforms such as phage, conjugative plasmids, mobile genomic islands, hydrogels, electroporation, and polymer-based nanoparticles have been utilized to deliver the CRISPR-Cas system.[51,52] In this study, we developed LNPs as a new platform, which we believe could hold potential for controlling bacterial infections using the CRISPR-Cas system if their versatility and efficiency can be improved.

This study provides initial evidence that LNPs can efficiently deliver nucleic acids into bacteria cells to induce bacterial cell death. However, the study has several limitations. First, we have no information on how LNPs facilitate the delivery of plasmids into bacteria and why the efficiency of LNP-assisted DNA delivery varies between bacterial species. Further work will be needed to determine the mechanism of delivery. Second, since the major "LNP-helper" polymyxin cannot work in polymyxin-resistant strains, a more versatile "LNP-helper" is needed. More natural "LNP-helpers" such as AMP, need to be evaluated. Third, while LNP-mediated delivery of CRISPR-Cas13a was effective in controlling bacterial infections in vivo, side effects in the animal model will need to be assessed. Nevertheless, this study provides important insights into the use of LNPs as a novel tool for the control of bacterial infection. The concept of an "LNP-helper" could promote further research into the development of new drug delivery systems. Moreover, new gRNA designs for AMR genes or virulence genes may provide a basis for the development of LNP-based gene therapy in the near future.

4. Experimental Section

LNP Screening Method for Bacteria: Lipids for LNPs were randomly combined and produced using the pipette mixing method (Table S1, Supporting Information). *E. coli* BW25113 was cultured in LB broth for 16 h at 37 °C, and then centrifuged. The cell pellet was resuspended in PBS (Sigma–Aldrich Co. St. Louis, MO, USA). *E. coli* BW25113 (2×10^9 CFU mL^{-1}) was treated with 1.5 μg mL^{-1} PMB using the "inverting" mix method. Subsequently, *E. coli* BW25113 (90 μL) and LNP (10 μL) were mixed and added to each well of a 96 multi-well plate and incubated for 4 h at 37 °C. The mixture (100 μL) was then spread on LB agar medium containing 50 μg mL^{-1} ampicillin (Sigma–Aldrich Co. St. Louis, MO USA). Colony forming units (CFU) were counted after 16 h of incubation at 37 °C. In the case of isolate no. 23, the experiment was conducted using the same method but with LB agar medium contained 50 μg mL^{-1} kanamycin (Sigma–Aldrich Co. St. Louis, MO USA).

Plasmid Constructions: pAD123::INR7 plasmids expressing EGFP were constructed and transformed into bacteria. EGFP fluorescence was detected on agar plates with an UV illuminator. For the construction of the high expression promoter, DNA fragments from *Bacillus pumilus* INR7[53] were randomly ligated into the pAD123 plasmid. Then, transformants expressing EGFP were selected. The pKLC21 vector, which carries the CRISPR-Cas13a system, was kindly provided by Dr. Longzhu Cui.[11,27] The pKLC21 vector expresses both Cas13a protein and gRNA, if the gRNA sequence is inserted. The plasmid pKLC21::16s carries both the Cas13a protein and the gRNA targeting the 16s rRNA gene of *Escherichia* spp. The gRNA was selected based on the sequence developed by Jonathan S. Gootenberg et al.[27] To construct pKLC21::16s, 33 mer oligo DNAs of crRNA-16s-as and crRNA-16s-s (which contain the BsaI restriction site) were synthesized and annealed in annealing buffer (10 mM Tris-HCl (pH 8.0), 50 mM NaCl, and 1 mM EDTA). Then, pKLC21 was cut with the restriction enzyme BsaI-HF and ligated with the annealed double-strand oligo DNA using T4 DNA ligase (Promega, USA). All primers used in this study are listed in Figure S8 (Supporting Information).

Preparation and Characteristic Analysis of LNPs: The LNP components were sourced from BroadPharm (San Diego, USA) with the following LNP codes (Table S1, Supporting Information). Lipidoid: 1, 2, 3, 4, 6, 7, 8, 9, 10, 11, 12, 13, 14, 15, 16, 17, 18, 19; Helper lipid: B, C, D, E, F; PEG-lipid: 4, 6, 7, 8, 9, 10. The LNP components from Avanti Polar Lipids Inc. (USA) have the following LNP codes. Lipidoid: 5; Helper lipid: A; PEG-lipid: 1, 2, 3, 5. The source of cholesterol was Sigma–Aldrich Co. The lipid to cargo weight ratio is included in the LNP code of Table S1 (Supporting Information). As a default, a lipid: cargo ratio of 10:1 was used in the LNP screening. All LNPs were prepared using the pipette mixing method. The diameters, zeta potential, and polydispersity index of lipid nanoparticles were measured at 20.0 °C by DLS using a Zetasizer Nano ZS90 (Malvern Instruments Ltd., Malvern, UK). The encapsulation efficiency of plasmids into LNPs was measured using Quant-iT PicoGreen dsDNA Assay Kit reagents and protocol (Thermo Fisher Scientific, Waltham, MA USA). The encapsulation efficiency was 76% for LNP 470 and 71% for LNP 496. For cryogenic electron microscopy (cryo-TEM), 3 μL of LNPs 470 or 496 was applied to Quantifoil holey carbon EM grids (R1.2/1.3, 200 mesh; EMS). The EM grids were glow-discharged for 60 s at 15 mA before sample application. Grids were blotted with Vitrobot Mark IV (FEI) using a 3 s blotting time with 100% relative humidity at 4 °C. Samples were imaged on Glacios (FEI) at an acceleration voltage of 200 kV with Falcon IV direct electron detector (FEI). Images were taken at 120 000 magnification with a defocus of –3.0 μm.

Rheological Analysis: Shear viscosity was measured using a rotational rheometer equipped with a cone and plate geometry (AR-G2, TA Instruments, diameter: 60 mm, angle: 1°, 20 °C) (Figure S2a, Supporting Information). Dimensionless capillary number,[54] defined as $\mathrm{Ca} = \frac{\mu_s \dot{\gamma} R_{\mathrm{LNP}}}{\sigma}$, where σ is the characteristic shear rate ($\dot{\gamma} = \frac{\langle u \rangle}{R}$) and the interfacial tension between LNP surface (LNP 470) and water, respectively. Since the LNP dimension is significantly smaller (Dynamic light scattering (DLS), $R_{\mathrm{LNP\,470}} = 67$ nm) and σ is an order of $O(10^2)$ Nm^{-1}, Ca is extremely small at $O(10^{-3})$, and thus deformation can be ruled out. In other words, LNP is estimated to be a hard-sphere colloidal dispersion. The measured viscosity data was applied to the Batchelor's equation[24] assuming a hard sphere model. $\eta_r = \eta_0/\eta_s = 1+2.5\phi_{eff}+5.9\phi_{eff}^2$ (η_r: relative viscosity, η_0: zero shear viscosity, η_0: zero shear viscosity, η_s: solvent viscosity, ϕ_{eff}: effective volume fraction). Solvent viscosity η_s was calculated as ≈1 cP for water at 20 °C.

Cell Viability Measurement: The human cervical squamous cancer cell line HeLa and the human embryonic kidney cell line HEK293T were grown in Dulbecco's modified Eagle's medium (DMEM, WelGENE Inc., Daegu, S. Korea) containing 10% fetal bovine serum (FBS, 16000–044, GIBCO, NY, USA), 100 U mL^{-1} penicillin, and 100 μg mL^{-1} streptomycin (Sigma–Aldrich Co. St. Louis, MO USA). The cells were grown in 25 or 75 T flasks in a 37 °C incubator with a humidified atmosphere of 5% CO_2. The cells (HeLa and HEK293T) were co-treated with LNPs and Lipofectamine 3000

(L3000008, Life Technologies, Carlsbad, CA, USA) together with 100 ng CleanCap EGFP mRNA (L-7601, TriLink BioTechnologies, CA, USA)/well for 24 h. Cell viability was measured using the D-Plus CCK kit (CCK-1000, Dongin, Seoul, South Korea) according to the manufacturer's instructions. The cells were incubated with the D-Plus CCK reagent (10 µL) for 2 h. Cell viability was determined using a microplate reader (Spark 10 M, Tecan, Zürich, Switzerland) at 450 nm.

Intracellular Delivery of LNPs Into Human Cell Lines: The animal cells (HeLa and HEK293T) were cultured in 24 multi-well plates at a density of 1×10^5 CFU mL^{-1} and pre-incubated for 24 h. The pre-incubated cells were transfected with 100 ng of mRNA using either Lipofectamine 3000 transfection reagent or LNPs. The fluorescence levels of the treated cells were analyzed using a CyFlow Cube 8 flow cytometer (Sysmex Partec, Görlitz, Germany). The relative fluorescence expression was determined by comparing the median fluorescence intensities of the treated cells. The median fluorescence intensities of the treated cells were calculated using FCS Express software (De Novo software, CA, USA).

LNP-Helper: Polymyxin B (PMB), polymyxin E (PME), ampicillin, and kanamycin were sourced from Sigma–Aldrich Co. In this study, antimicrobial peptide (AMP1, 2, & 3) samples (unpublished) from Peptide Engineering Laboratory at Chosun University were utilized. AMP4 (Oligopeptide-76, JForCell, South Korea), AMP5 (Aurein 1.2, JForCell, South Korea), and 2-(4-chlorophenyl)−6-methyl-4-nitrophenol (PA108)[22] were also used.

Evaluation of Protective Effect Against Mouse Sepsis Model: The animal experimental study was conducted in compliance with the approved experimental program of the Animal Care and Use Committee at the Korea Research Institute of Bioscience and Biotechnology (Approval No. 22139). Female C57BL/6J mice, aged six weeks and pathogen free, were obtained from Daehan Biolink Corporation, Kiheung city, Korea. Upon arrival, the mice underwent a quarantine period, followed by a seven-day acclimation period before being separated into individual groups. Throughout the entire experiment, the mice were housed in a room with controlled temperature (20.5–23.0 °C) and humidity (36-56%). They were kept in stainless mesh cages with wood bedding, with three mice per cage. A clinical isolate of *Escherichia fergusonii* was utilized to assess the efficiency of LNP treatment against intraperitoneal infection. Thirty mice were randomly divided into three groups, as follows; 1, an infected alone control group; 2, an infected and LNP- encapsulated pKLC21 plasmid vector treatment group; 3, an infected and LNP-encapsulated pKLC21::16s rRNA treatment group. Each group was administered *E. fergusonii* at 2×10^8 CFU per mice intraperitoneally, followed by intraperitoneal treatment with the respective LNP within 3 min after the infection. 100 µL of buffered saline was used to treat the infected alone control animals. Clinical signs and survival rates were monitored for a duration of up to 80 h post-infection.

Galleria Mellonella Time Kill Assay: To compare the virulence of the 15 clinical isolates, *Galleria mellonella* caterpillars were infected with each isolate. All strains used in this study are listed in Figure 4. Isolates cultivated in LB medium for 16 h at 37 °C were washed with PBS and diluted. Then, 10 µL of culture (1.0×10^9 CFU μL^{-1}) was injected into *G. mellonella* (n = 10) using insulin syringes (BD Ultra-Fine II Short Needle Syringes, 0.3 mL). Infected caterpillars were kept in a 37 °C incubator and survival rate was determined after 48 h. For evaluation of LNP delivery in vivo, *G. mellonella* caterpillars were infected with a mixture of the clinical isolate No. 23 (*Escherichia fergusonii*) and LNP. Bacterial cells cultivated in LB medium for 16 h at 37 °C were washed with PBS. Bacterial cells were pretreated with 2 µg mL^{-1} PMB before infection as described in the PMB pretreatment method. For infection, 90 µL of PMB-treated bacterial cells (1.2×10^9 CFU μL^{-1}) and 10 µL of LNP were mixed in a 96 multi-well plate. Then, 10 µL of the mixture was injected into *G. mellonella* ($n = 10$) using insulin syringes. Infected caterpillars were kept in a 37 °C incubator to determine survival after 48 h.

Statistical Analysis: Statistical analysis of all the experiments was determined using Prism 9 software (GraphPad). For the bar diagram, the error bars indicate the mean ± SD. Sample sizes were indicated in figure captions. Significance between two groups and between multiple groups were assessed by a two-tailed unpaired Student's *t*-test and one-way ANOVA followed by Dunnett's multiple comparisons test, respectively. Survival comparison was performed using the Log-rank (Mantel-Cox) test. Differences were determined as statistically significant with a *P* value < 0.05. $^{*}p < 0.05$; $^{**}p < 0.01$; $^{***}p < 0.001$; $^{****}p < 0.0001$; ns, not significant.

Compliance with Ethics Requirement: The animal study was conducted following the experimental protocol approved by the Institute Animal Care and Use Committee at the Korea Research Institute of Bioscience and Biotechnology (No. AEC-23173).

Supporting Information

Supporting Information is available from the Wiley Online Library or from the author.

Acknowledgements

The authors are grateful to Dr. Longzhu Cui and Kotar Kiga (Jichi Medical University, Tochigi, Japan) for providing the pKLC21 vector encoding Cas13a, which contains the cloning site for gRNA. The authors thank the Core Facility Management Center at the Korea Research Institute of Bioscience and Biotechnology (KRIBB) for assistance with cryoEM. This research was supported by the Bio&Medical Technology Development Program of the National Research Foundation (NRF) funded by the Korean government (MSIT) (No. RS-2023-00219213) and the Korea Research Institute of Bioscience and Biotechnology (KRIBB) Research Initiative Program.

The authors thank Dr. Yoonkyung Kim (KRIBB, Daejeon, South Korea) for providing the LNP of the Moderna vaccine combination.

[Correction added on 6 February 2025 after first online publication: Acknowledgement Section has been updated.]

Conflict of Interest

B.K., D.K., and C.M.R. have filed patent applications based on the methods described in this report.

Data Availability Statement

The data that support the findings of this study are available in the supplementary material of this article.

Keywords

alternative antibiotics, bacterial infection, Cas13a, CRISPR-cas system, lipid nanoparticles, nucleic acids delivery

Received: August 31, 2024
Revised: November 10, 2024
Published online: November 24, 2024

[1] J. Hsu, *BMJ* **2020**, *369*, m1983.
[2] T. M. Rawson, D. Ming, R. Ahmad, L. S. Moore, A. H. Holmes, *Nat. Rev. Microbiol.* **2020**, *18*, 409.
[3] A. R. Mahoney, M. M. Safaee, W. M. Wuest, A. L. Furst, *iScience* **2021**, *24*, 102304.
[4] C. Årdal, M. Balasegaram, R. Laxminarayan, D. McAdams, K. Outterson, J. H. Rex, N. Sumpradit, *Nat. Rev. Microbiol.* **2020**, *18*, 267.
[5] X. Cui, Y. Lü, C. Yue, *Infect. Drug Resist.* **2021**, *14*, 5575.
[6] C. F. Carson, T. V. Riley, *Commun. Dis. Intell.* **2003**, *27*, S143.
[7] J. A. Kulkarni, D. Witzigmann, S. B. Thomson, S. Chen, B. R. Leavitt, P. R. Cullis, R. van der Meel, *Nat. Nanotechnol.* **2021**, *16*, 630.

[8] F. Depardieu, D. Bikard, *Methods* **2020**, *172*, 61.
[9] K. Selle, J. R. Fletcher, H. Tuson, D. S. Schmitt, L. McMillan, G. S. Vridhambal, A. J. Rivera, S. A. Montgomery, L.-C. Fortier, R. Barrangou, *MBio* **2020**, *11*, e00019.
[10] O. O. Abudayyeh, J. S. Gootenberg, P. Essletzbichler, S. Han, J. Joung, J. J. Belanto, V. Verdine, D. B. Cox, M. J. Kellner, A. Regev, *Nature* **2017**, *550*, 280.
[11] K. Kiga, X.-E. Tan, R. Ibarra-Chávez, S. Watanabe, Y. Aiba, Y. Sato'o, F.-Y. Li, T. Sasahara, B. Cui, M. Kawauchi, *Nat. Commun.* **2020**, *11*, 2934.
[12] X.-Y. Xue, X.-G. Mao, Y. Zhou, Z. Chen, Y. Hu, Z. Hou, M.-K. Li, J.-R. Meng, X.-X. Luo, Medicine, *Nanomed.-Nanotechnol. Biol. Med.* **2018**, *14*, 745.
[13] S. Tarvirdipour, M. Skowicki, C.-A. Schoenenberger, C. G. Palivan, *Int. J. Mol. Sci.* **2021**, *22*, 9092.
[14] G. C. Kim, D. H. Cheon, Y. Lee, *Biochim. Biophys. Acta Proteins Proteomics* **2021**, *1869*, 140604.
[15] A. J. Barbier, A. Y. Jiang, P. Zhang, R. Wooster, D. G. Anderson, *Nat. Biotechnol.* **2022**, *40*, 840.
[16] S. Meo, I. Bukhari, J. Akram, A. Meo, D. C. Klonoff, *Eur. Rev. Med. Pharmacol. Sci.* **2021**, *25*, 1663.
[17] P. Cullis, P. Felgner, *Nat. Rev. Drug. Discovery.* **2024**, *23*, 709.
[18] K. L. Swingle, A. G. Hamilton, M. J. Mitchell, *Trends Mol. Med* **2021**, *27*, 616.
[19] J. Sun, S. T. Rutherford, T. J. Silhavy, K. C. Huang, *Nat. Rev. Microbiol.* **2022**, *20*, 236.
[20] S. Halder, K. K. Yadav, R. Sarkar, S. Mukherjee, P. Saha, S. Haldar, S. Karmakar, T. Sen, *SpringerPlus* **2015**, *4*, 672.
[21] A. Khondker, M. C. Rheinstädter, *Commun. Biol.* **2020**, *3*, 77.
[22] S.-Y. Kim, H. W. Seo, M.-S. Park, C. M. Park, J. Seo, J. Rho, S. Myung, K. S. Ko, J.-S. Kim, C.-M. Ryu, *J. Antimicrob. Chemother.* **2023**, *78*, 923.
[23] M. Schlich, R. Palomba, G. Costabile, S. Mizrahy, M. Pannuzzo, D. Peer, P. Decuzzi, *Bioeng. Transl. Med.* **2021**, *6*, e10213.
[24] W. B. Russel, D. A. Saville, W. R. Schowalter, *Colloidal Dispersions*, Cambridege **1989**.
[25] B. Kim, S. S. Lee, T. H. Yoo, S. Kim, S. Y. Kim, S.-H. Choi, J. M. Kim, *Sci. Adv.* **2019**, *5*, eaav4819.
[26] R. Ala-Jaakkola, A. Laitila, A. C. Ouwehand, L. Lehtoranta, *Nutr. J.* **2022**, *21*, 18.
[27] J. S. Gootenberg, O. O. Abudayyeh, J. W. Lee, P. Essletzbichler, A. J. Dy, J. Joung, V. Verdine, N. Donghia, N. M. Daringer, C. A. Freije, *Science* **2017**, *356*, 438.
[28] K. Kiga, X.-E. Tan, R. Ibarra-Chávez, S. Watanabe, Y. Aiba, Y. Sato'o, F.-Y. Li, T. Sasahara, B. Cui, M. Kawauchi, T. Boonsiri, K. Thitiananpakorn, Y. Taki, A. H. Azam, M. Suzuki, J. R. Penadés, L. Cui, *Nat. Commun.* **2020**, *11*, 2934.
[29] E. Kon, U. Elia, D. Peer, *Curr. Opin. Biotechnol.* **2022**, *73*, 329.
[30] J. Witten, Y. Hu, R. Langer, D. G. Anderson, *Proc. Natl. Acad. Sci. USA* **2024**, *121*, e2307798120.
[31] M. K. Jeengar, M. Kurakula, P. Patil, A. More, R. Sistla, D. Parashar, *Molecules* **2022**, *27*, 1170.
[32] R. C. Steffens, E. Wagner, *Pharm. Res.* **2023**, *40*, 47.
[33] L. Zhang, S. Wu, Y. Qin, F. Fan, Z. Zhang, C. Huang, W. Ji, L. Lu, C. Wang, H. Sun, *Nano Lett.* **2019**, *19*, 4237.
[34] A. S. Dossou, M. E. Mantsch, A. Kapic, W. L. Burnett, N. Sabnis, J. L. Coffer, R. E. Berg, R. Fudala, A. G. Lacko, *Pharmaceutics* **2023**, *15*, 1685.
[35] P. R. Taylor, S. Gordon, L. Martinez-Pomares, *Trends Immunol.* **2005**, *26*, 104.
[36] L. F. García-Alles, A. Zahn, B. Erni, *Biochemistry* **2002**, *41*, 10077.
[37] J.-M. Jeckelmann, B. Erni, *Biochim. Biophys. Acta-Biomembr.* **2020**, *1862*, 183412.
[38] C. S. Hung, J. Bouckaert, D. Hung, J. Pinkner, C. Widberg, A. DeFusco, C. G. Auguste, R. Strouse, S. Langermann, G. Waksman, *Mol. Microbiol.* **2002**, *44*, 903.
[39] J. Bouckaert, J. Berglund, M. Schembri, E. De Genst, L. Cools, M. Wuhrer, C. S. Hung, J. Pinkner, R. Slättegård, A. Zavialov, *Mol. Microbiol.* **2005**, *55*, 441.
[40] S. Manioglu, S. M. Modaresi, N. Ritzmann, J. Thoma, S. A. Overall, A. Harms, G. Upert, A. Luther, A. B. Barnes, D. Obrecht, *Nat. Commun.* **2022**, *13*, 6195.
[41] Y. Huan, Q. Kong, H. Mou, H. Yi, *Front. Microbiol.* **2020**, *11*, 582779.
[42] Q.-Y. Zhang, Z.-B. Yan, Y.-M. Meng, X.-Y. Hong, G. Shao, J.-J. Ma, X.-R. Cheng, J. Liu, J. Kang, C.-Y. Fu, *MILITARY MED. RES.* **2021**, *8*, 48.
[43] A. Steimle, I. B. Autenrieth, J.-S. Frick, *Int. J. Med. Microbiol.* **2016**, *306*, 290.
[44] B. D. Needham, M. S. Trent, *Nat. Rev. Microbiol.* **2013**, *11*, 467.
[45] Z. Zhou, S. Lin, R. J. Cotter, C. R. Raetz, *J. Biol. Chem.* **1999**, *274*, 18503.
[46] K. K. Cooper, R. E. Mandrell, J. W. Louie, J. Korlach, T. A. Clark, C. T. Parker, S. Huynh, P. S. Chain, S. Ahmed, M. Q. Carter, *BMC Genomics* **2014**, *15*, 17.
[47] F. Ran, P. D. Hsu, J. Wright, V. Agarwala, D. A. Scott, F. Zhang, *Nat. Protoc.* **2013**, *8*, 2281.
[48] P. Wan, S. Cui, Z. Ma, L. Chen, X. Li, R. Zhao, W. Xiong, Z. Zeng, *Infect. Drug Resist.* **2020**, *13*, 1171.
[49] P. Wang, D. He, B. Li, Y. Guo, W. Wang, X. Luo, X. Zhao, X. Wang, *J. Antimicrob. Chemother.* **2019**, *74*, 2559.
[50] G. Ram, H. F. Ross, R. P. Novick, I. Rodriguez-Pagan, D. Jiang, *Nat. Biotechnol.* **2018**, *36*, 971.
[51] E. Bier, V. Nizet, *Trends Genet.* **2021**, *37*, 745.
[52] Y. Wu, D. Battalapalli, M. J. Hakeem, V. Selamneni, P. Zhang, M. S. Draz, Z. Ruan, *J. Nanobiotechnol.* **2021**, *19*, 401.
[53] H. Jeong, S.-K. Choi, J. W. Kloepper, C.-M. Ryu, *Genome Ann* **2014**, *2*, 01093.
[54] D. Pan, N. Phan-Thien, B. C. Khoo, *J. Non-Newton. Fluid Mech.* **2014**, *212*, 63.